Towards a new Structural Imaging Package (STIP)

Jan Thorbecke [1]
A.J. Berkhout [2]

12.1 Introduction

In chapter 10 migration is described in terms of double focussing. In chapter 11 focussing in emission is used to synthesize common focus point gathers (CFP gathers). By comparing a CFP-gather with its related focussing operator velocity errors can be detected and the focussing operator can be corrected (Berkhout and Rietveld (1994), Rietveld and Berkhout (1994) , Berkhout (1992), Rietveld and Thorbecke (1994)). Next the CFP gather can be stacked, yielding one sample of the prestack migration result. We have designed a new structural imaging package (STIP) based on the CFP technology. In this chapter some practical aspects are discussed.

12.2 Description of the STIP package

The common focus point gather is build on **all** seismic data within a pre-specified aperture. To construct the CFP-gather an initial synthesis operator is needed. This initial synthesis operator can be based on a homogeneous model (if very little information is available), stacking velocities or an initial macro model. In principle the first synthesis operator is chosen in such a way that the focus point is positioned near the shallowest macro boundary. After the synthesis process the synthesis operator can be compared with the constructed CFP-gather. Now the strongest reflection is chosen near the operator. Picking is done in an interactive way by mouse tracking the desired event. With this selection an unknown focus point is defined at a (strong) reflector near the specified focus point. The mismatch between the synthesis operator and the selected

[1]E-mail: J.W.Thorbecke@CTG.TUDelft.NL
[2]E-mail: A.J.Berkhout@CTG.TUDelft.NL

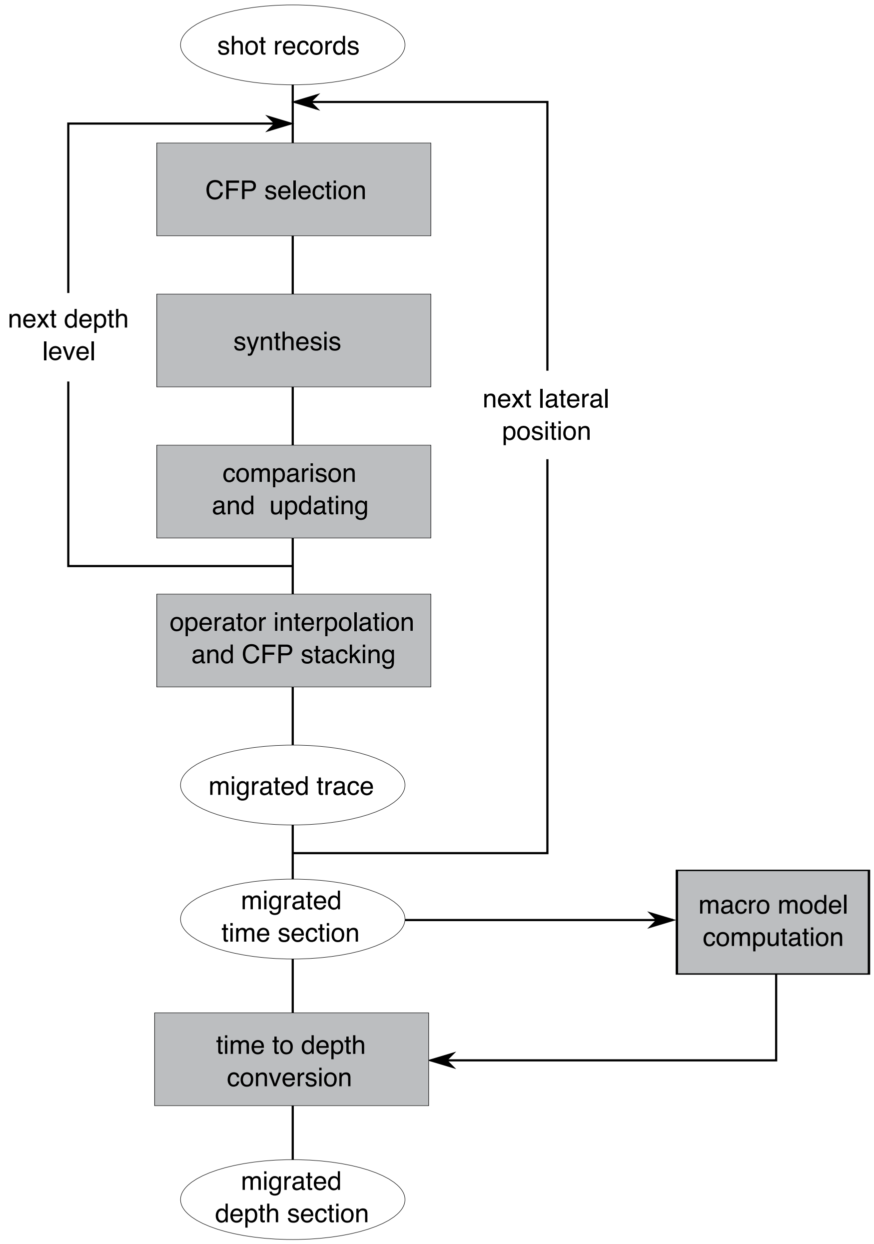

Fig. 12.1 *CFP processing scheme. Note that the migrated time section (in one-way time) is obtained without using a macro model.*

event can be corrected by means of a simple iterative procedure which will be explained below. After one or two iterations the synthesis operator and the CFP-gather contain exactly the same event. Weighted stacking of the CFP gather with the aid of the synthesis operator gives a pre-stack image which is correct for the related focus point response. By selecting more focus points in the subsurface (at the same lateral position) more imaging results can be calculated. We propose a top-down approach: from shallow to deep. The previous operator can be used as initial estimate for the next one. The same process can be repeated for other lateral positions. Finally we will have many synthesis operators scattered over the x-t section of the seismic line.

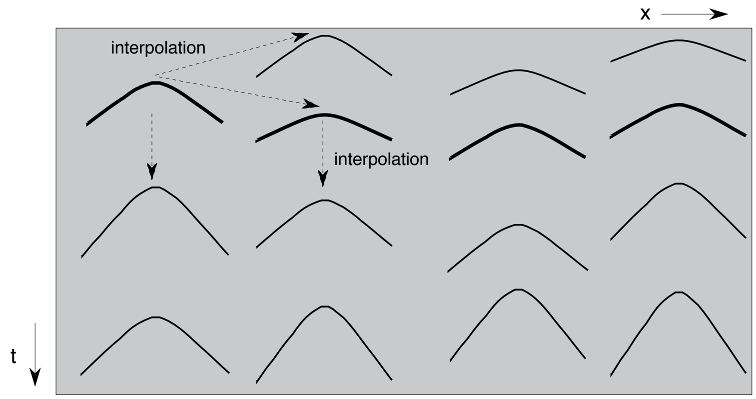

Fig. 12.2 *Collection of synthesis operators as a result of the scheme in Figure 12.1. Intermediate synthesis operators are obtained by interpolating between the given operators. Note that this collection of synthesis operators is an excellent starting point for macro model estimation.*

This collection of synthesis operators is schematically shown in Figure 12.2. Using this collection of synthesis operators and intermediate operators, obtained by interpolating in between the given operators, a time image of the subsurface can be built up without using a macro model. To convert this time image to a structural model (depth image) a macro model is needed. This macro model can be estimated by using the collection of synthesis operators and the obtained time image.

The basic steps in the STIP package can be summarized as follows (Figure 12.1):

1. Selection of the first focus point; start in a good data area. Compute the focussing areal source, e.g. by using a stacking velocity model.
2. Synthesize the related CFP-gather.
3. (a) Compare of time-reversed focussing areal source and the related CFP-gather; update the areal source to its correct version and store the correct operator.
   (b) Optional: cross correlation of focussing areal source with CFP-gather (resolution analysis).
   (c) Optional: AVO analysis.
4. Repeat for a number of focus points at the same lateral position (top-down approach).
5. Interpolate the relatively sparse focussing areal sources to obtain CFP-stacking operators at each time sample.
6. Compute the CFP-stack, yielding one trace of the migration output in one-way time.
7. Repeat for all lateral positions; use focussing operators of the previous lateral position as an initial estimate for the next lateral position.
8. Compute the macro velocity model from all operators; derive the initial boundaries from the migration result.
9. Apply a one-way-time to depth conversion.

The central role of the CFP gather in the proposed method demands a further examination of the properties of the CFP gather. Therefore some interesting properties of the common focus point gathers are described below.

Groundroll and direct wave

The linear events in a seismic shot record, the direct wave and the (dispersive) groundroll, are the low velocity events that we don't want to have in our CFP gathers. However, after the synthesis process these events have a small contribution in the relevant part of the CFP-gather due to their low apparent velocities. This is illustrated in Figure 12.3. In this example we have used three different synthesis operators that have their focus points at 100, 200 and 400 meter below the surface. At the surface of the model we have inserted a layer with a vertical gradient to make the surface waves dispersive.

In Figure 12.3d the linear events, processed by the synthesis operator, have only a contribution in the CFP gather close to zero time. If the focus point is chosen deeper the effects of the direct wave and the groundroll are shifted to 'negative' times. In this way the linear near surface effects are not disturbing the important part of the CFP gather, which is the event where the focus point operator is designed for. In the CFP gather for the deepest focus point in Figure 12.3h the groundroll and the direct wave are completely absent and comparison of the CFP gather with the synthesis operator is not disturbed by these events. The important effect of aliasing is under study.

12.3 Examples

In this section two examples are described which will further clarify the concepts of the proposed structural imaging technique. In the first subsection, in which a 1D multi-layer medium is taken, the imaging of CFP gathers is explained. The second subsection tests the comparison of the synthesis operator with the CFP-gather by placing a complicated weathered layer on top of a one reflector model.

12.3.1 1-Dimensional multi-layer

The 1-dimensional multi layer model is based on an impedance log and is shown in Figure 12.4a. To illustrate the imaging procedure of CFP gathers two focus points are chosen in the subsurface; one at the sea bottom and another one at a depth of approximately 1800 m (in the neighborhood of the strong reflector). The initial synthesis operators are chosen such that they are close to the half-way time of the event of interest. This is done by modelling a 2 dimensional Green's functions in a homogeneous medium for a source position at 300 m (for the sea bottom) and 1800 m (for the deep reflector). Note that these initial synthesis operators do not take into account the propagation effects of the layers above the defined focus point.

Within one iteration of the updating process, which was described above, the travel time curve

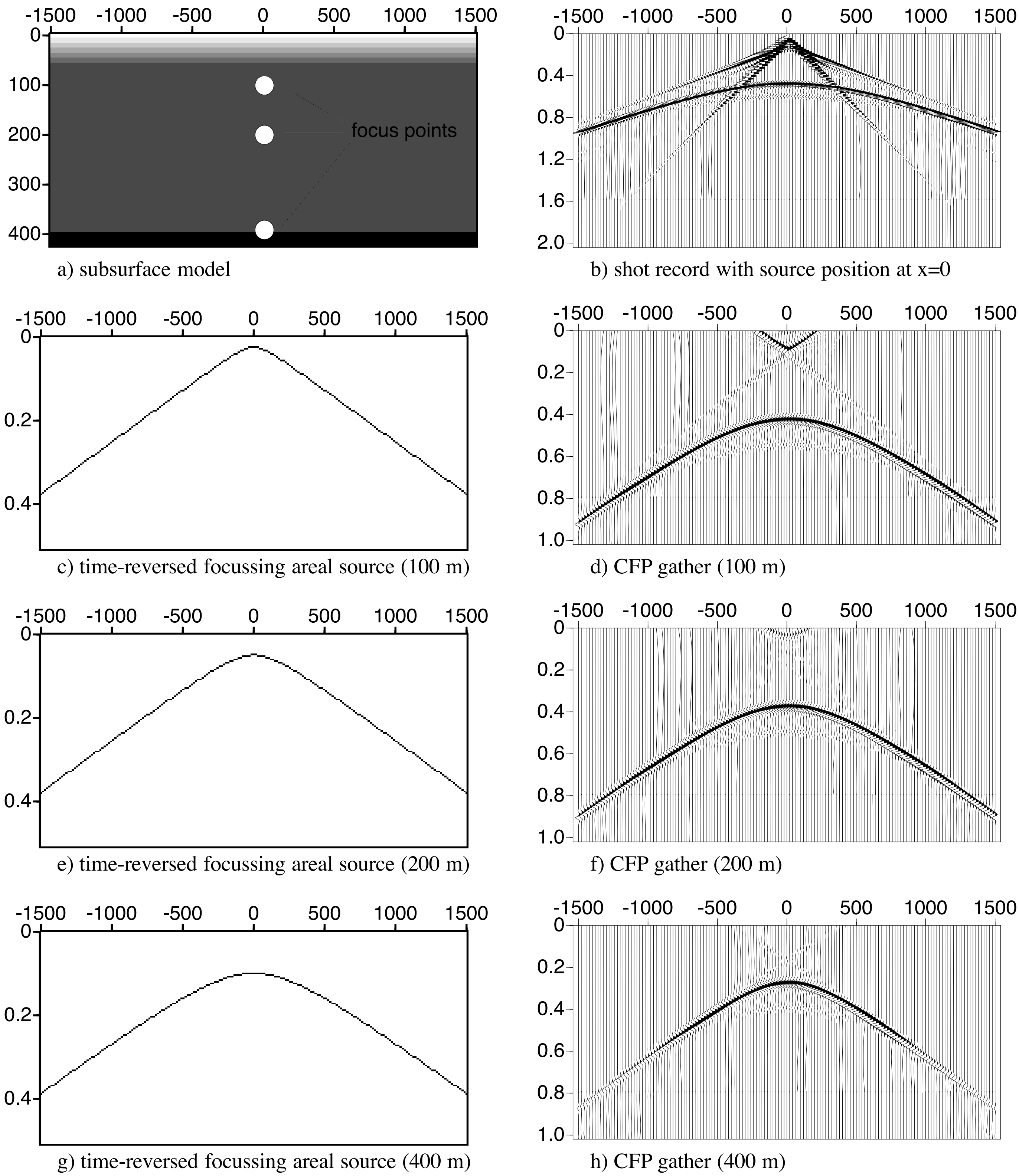

a) subsurface model

b) shot record with source position at x=0

c) time-reversed focussing areal source (100 m)

d) CFP gather (100 m)

e) time-reversed focussing areal source (200 m)

f) CFP gather (200 m)

g) time-reversed focussing areal source (400 m)

h) CFP gather (400 m)

Fig. 12.3 *Removal of surface waves (direct wave and dispersive groundroll) by synthesizing common focus point gathers for focus points below the weathered layer.*

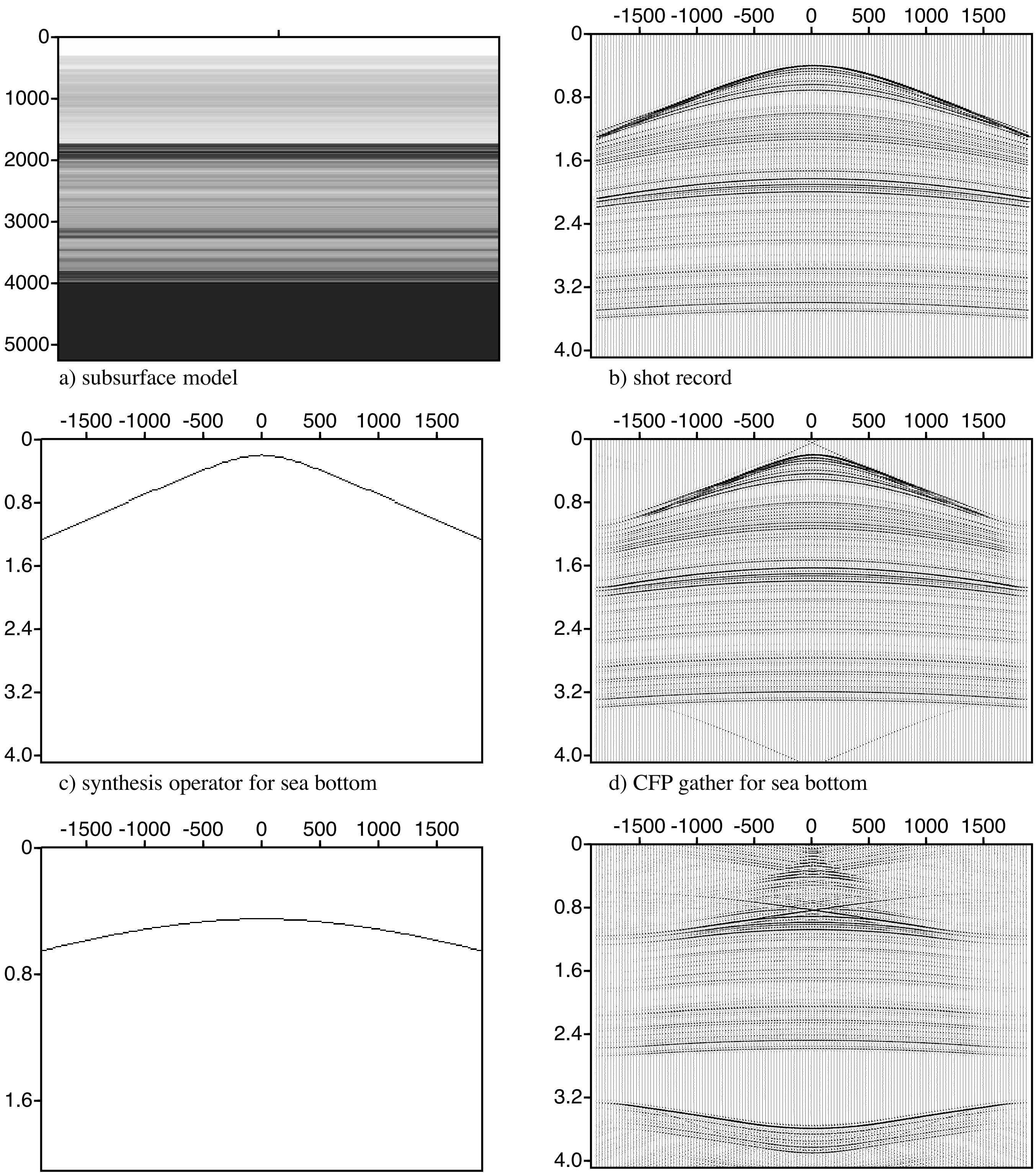

a) subsurface model

b) shot record

c) synthesis operator for sea bottom

d) CFP gather for sea bottom

e) synthesis operator for deep reflector

f) CFP gather for deep reflector

Fig. 12.4 *Operators and CFP gathers for a 1 dimensional multi layer example with a focus point at the sea bottom and a focus point at a deep reflector at 1800 m. After one iteration the correct operators were obtained.*

of the synthesis operator coincides with the travel time curve of the selected event in the CFP gather.

12.3.2 One deep plane reflector with weathered layer (2D)

The iterative updating of the synthesis operator enables us to take all the geometrical propagation effects into account. How good this can be done is tested by taking a low velocity layer close to the surface of the model and a flat reflector 400 m below the surface. If the matching

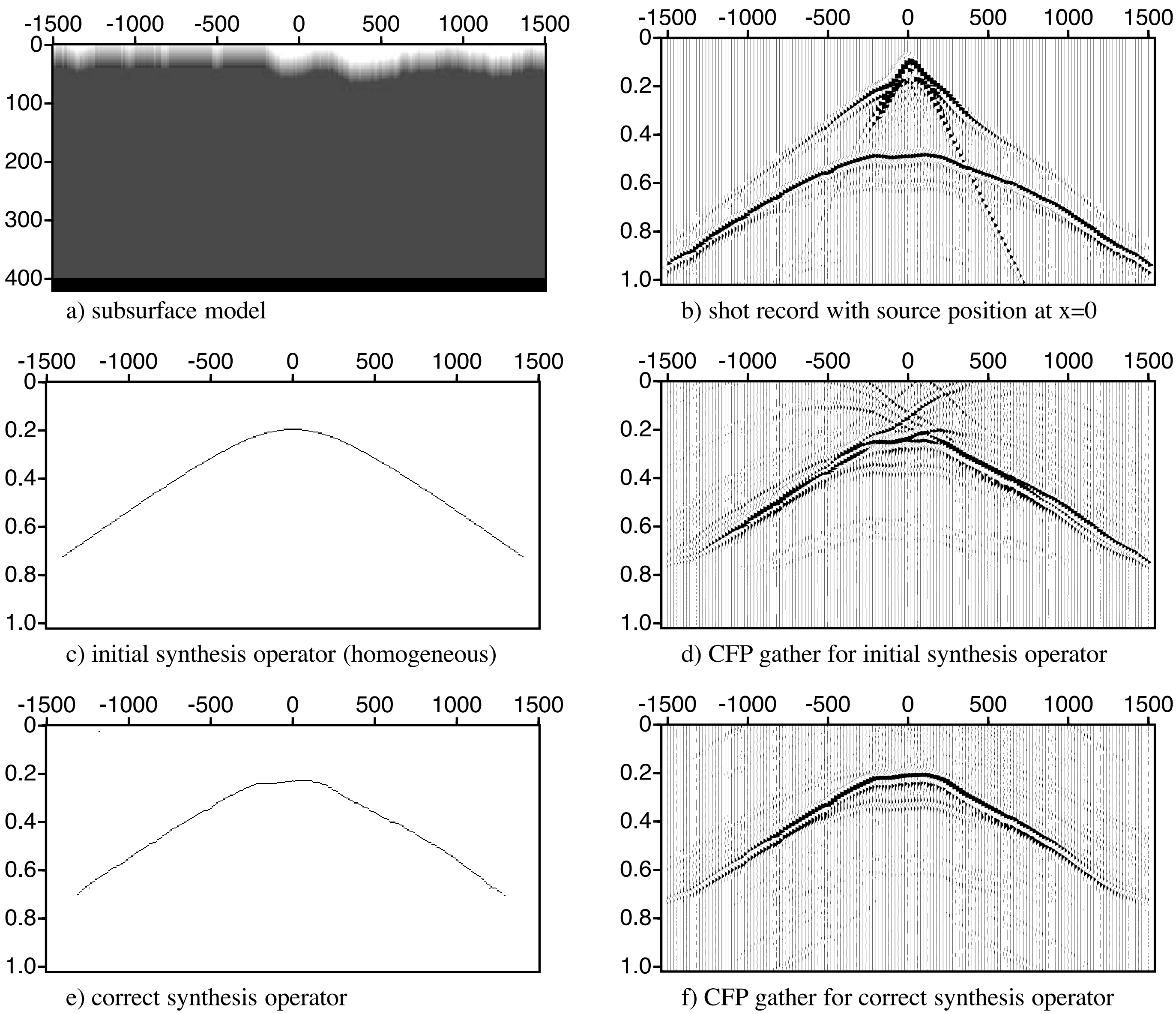

Fig. 12.5 *Operators and CFP gathers for a deep reflector with a weathered layer on top. Weighted stacking of the CFP gather, using the synthesis operator, yields the correct migration result for the double focus point.*

of the synthesis operator with the selected event (the deep reflector) is correct then the operator of the deeper layer should come out correctly including the one-way disturbing effects of the weathered layer. The model is shown in Figure 12.5a and a shot record, with a source position at the surface positioned in the centre of the model (x=0), is shown in Figure 12.5b. Note the irregular shaped 'hyperbola' of the deeper reflector.

The initial synthesis operator is a pulse response of a source at 400 m depth in a homogeneous medium with a velocity of 2000 m/s as given in Figure 12.5c. The CFP gather processed with this synthesis operator is shown in Figure 12.5d. Note the mismatch between the synthesis operator and the CFP gather. This mismatch is used to iterate to the correct operator. By taking the correct synthesis operator of Figure 12.5e the constructed CFP gather is identical in travel-time with the synthesis operator and focussing in detection may now occur.

12.4 Updates for mismatch

In DELPHI, volume V Chapter 11, (1994) we have tried to derive update formula's for depth and velocity errors in a 1 dimensional macro model. We have shown that it is possible to derive a closed form solution of the update formula in case of a one layer model and a depth error. For other errors and more complicated models we could not derive closed form solutions. However, using the theory in chapter 11 a principally different approach can be followed. Given an initial synthesis operator, it is **not** necessary to find an event in the CFP gather that 'belongs to' the operator. Any suitable event close to the operator may be chosen. The truth is 'in the middle' (principle of equal complexity). This insight may be seen as a fundamental breakthrough for the pre-stack migration process, particularly in complex situations. To illustrate this, assume a hyperbolic time behavior for the initial synthesis operator (T_s^0) and the synthesized shot record (T_d) yields

$$T_s^0(x) = \frac{\sqrt{z_s^2 + (x - x_0)^2}}{c_s} \tag{12.1}$$

$$T_d(x) = \frac{\sqrt{z_d^2 + (x - x_0)^2}}{c_d} \tag{12.2}$$

with z_s the depth of the focus point , c_s an average velocity, x_0 the lateral position of the source and x a receiver position. $T_s^0(x)$ describes the time behavior of the initial synthesis operator and $T_d(x)$ describes the time behavior of the CFP gather. The update of the synthesis operator is given by

$$T_s^1(x) = T_s^0(x) + T_c(x) \tag{12.3}$$

where $T_c(x)$, a function of $T_d(x) - T_s^0(x)$, is the update we are looking for. By choosing $T_c(x) = \frac{T_d(x) - T_s^0(x)}{2}$ the update is correct $x = x_0$ but for larger offsets the update is less accurate, therefore a second iteration step is needed to correct the mismatch in the larger offsets. In Figure 12.6 two examples out of Chapter 11 are used to demonstrate the convergence of the linear update scheme. The used examples contain a depth or a velocity error in the synthesis operator for a

1D model with one layer. Although the initial macro model and the CFP gather are different in both examples they converge to the same answer within two iterations. This validates the very fast convergence of the iterative scheme and shows that only a very few iterations are needed to converge to the final answer.

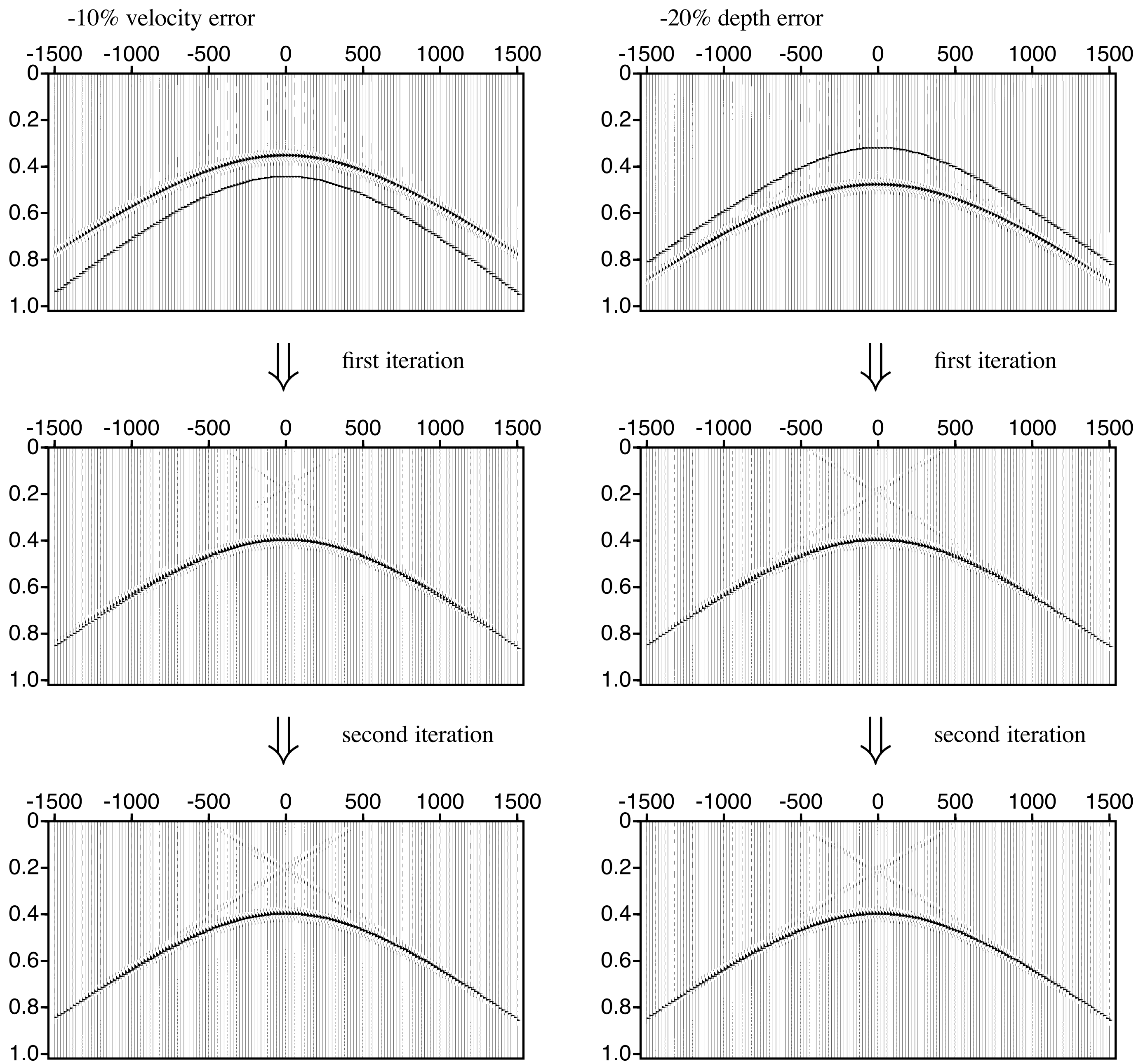

Fig. 12.6 *Synthesis operator updating with linear updating algorithm. Note that both CFP gathers converge very fast to the same CFP gather with a focus point on the reflector. One iteration is sufficient.*

12.5 Removal of finite aperture artefacts

In the synthesis process every shot record is transformed to the frequency domain and multiplied with the synthesis operator. The multiplication in the frequency domain can be regarded as an one way inverse extrapolation step. The result of this multiplication is summed over all receivers in the shot record to produce one trace of the CFP gather. Wapenaar (1991) has showed that due to the finite aperture of the data, artefacts are introduced in this final result. These artefacts can be suppressed by using a taper at the edges of the data set. But tapering only suppresses the artefacts (and a part of the data as well) and does not remove the artefacts. Therefore Wapenaar (Timmerman (1993)) proposed a new technique to calculate the artefacts originating from the finite aperture and subtract these from the data. This method can be very useful in obtaining

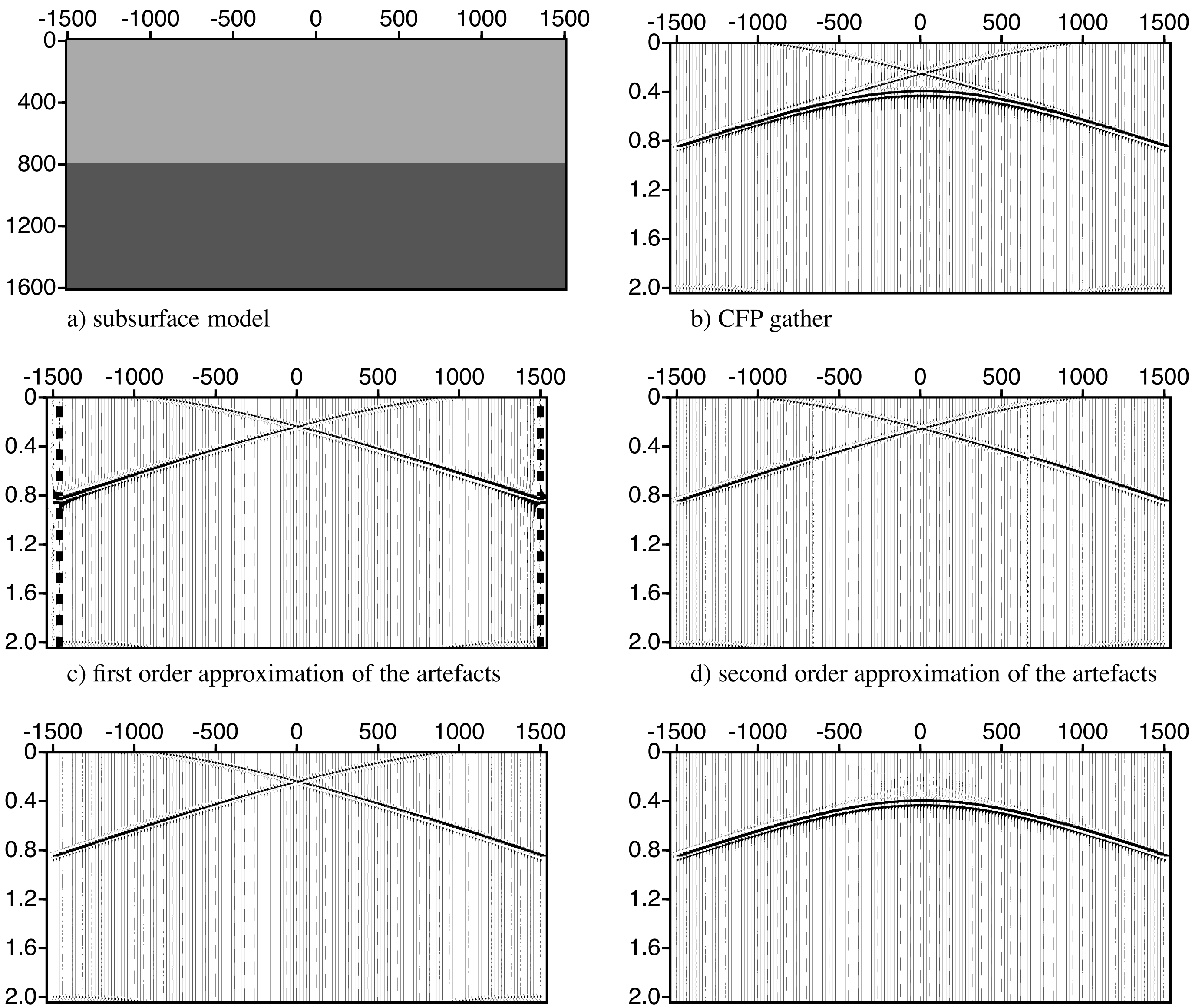

a) subsurface model
b) CFP gather
c) first order approximation of the artefacts
d) second order approximation of the artefacts
e) combination of first and second order approximation
f) CFP gather with removal of the artefacts in (e)

Fig. 12.7 *Finite aperture artefacts removal in the CFP gather. Note that all figures are plotted on the same scale.*

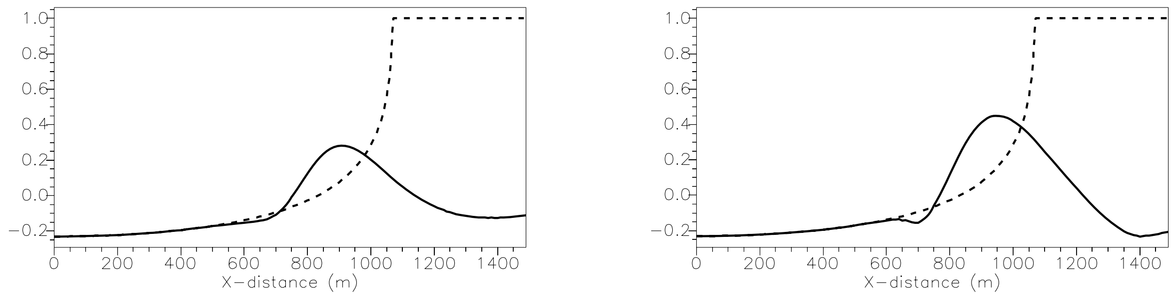

a) AVO curve without finite aperture removal   b) AVO curve with finite aperture removal

Fig. 12.8 *AVO behavior and finite aperture artefacts removal in the CFP gather.*

better AVO information and suppression of the artefacts. The summation over all shot records, to obtain one trace in the CFP gather, can be represented by the following integral

$$I = \int_{-\infty}^{\infty} f(x) e^{j\phi(x)} dx \tag{12.4}$$

where $f(x)$ and $\phi(x)$ represent the amplitude and phase, respectively. Due to the finite acquisition aperture equation (12.5) is approximated by

$$< I >= \int_{x_a}^{x_b} f(x) e^{j\phi(x)} dx \tag{12.5}$$

where x_a and x_b are the begin- and end-points of the acquisition aperture. These finite integration limits cause artefacts. Wapenaar expresses the correct result I in terms of the approximated result $< I >$ plus two correction terms, as follows:

$$I =< I > +I_a + I_b \tag{12.6}$$

where

$$I_a = \int_{-\infty}^{x_a} f(x) e^{j\phi(x)} dx \tag{12.7}$$

and

$$I_b = \int_{x_b}^{\infty} f(x) e^{j\phi(x)} dx \tag{12.8}$$

By adding I_a and I_b to the processing result we expect to compensate fully for the diffraction artefacts. The method of Wapenaar makes a first and second order approximation to the finite aperture artefacts described in equations (12.5) (12.5). If first order approximation breaks down the second order approximation should be used. In Figure 12.7b a CFP gather is shown for one reflector with a reflection coefficient constant for all angles of incidence (only a density contrast). Note that the artefact which starts on the lower left side of Figure 12.7a disturbs the event at the right side.

In Figure 12.7c the first order approximation of the finite aperture artefact is shown. Note that the approximation breaks down for the far offsets. The second order approximation of the artefact is shown in Figure 12.7d. Note that the approximated artefact is wrong for small offsets. A combination of the first and second order approximation is easily made and shown in Figure 12.7e. Subtracting these artefacts from Figure 12.7b gives the artefacts free result of Figure 12.7f. In Figure 12.8 AVO curves are shown with and without finite aperture removal applied. The same example shown in Chapter 10 and 11 is used again. The improvement of the AVO curve is clear from Figure 12.8b; for larger offset the curve follows the analytical curve better.

12.6 Discussion and Future plans

The examples in this chapter have demonstrated some of the very favorable properties of the CFP gather technology in macro model estimation and structural imaging. With the common focus point technique it is possible to get a pre-stack structural image in **one-way** time without knowing a macro model; also an AVO analysis process can be applied. The truncation artefacts, present in the CFP gather, are disturbing the accuracy of the AVO near the edges of the aperture. This can be improved by removal of these artefacts as proposed by Wapenaar (1991).

In the near future we will implement the proposed CFP imaging technique in a interactive processing environment. In this package the user will guide the automatic tracking in a CFP-gather. The updating of a synthesis operator and its related CFP gather will be computed automatically within a few seconds so the user is able to work fast. The collection of (selected) synthesis operators that are generated during the structural imaging process will be used to estimate the macro model by a one-way tomographic inversion process.

12.7 References

Berkhout, A. J., and Rietveld, W. E. A., 1994, Determination of macro models for prestack migration; part 1 estimation of macro velocities: 64th Ann. Internat. Mtg., SEG, Expanded Abstracts, SM6.2; 1330–1333.

Berkhout, A. J., 1992, Pushing the limits of seismic imaging: 62th Ann. Internat. Mtg., SEG, Expanded Abstracts, W–4; 1389–1393.

Rietveld, W. E. A., and Berkhout, A. J., 1994, Determination of macro models for prestack migration; part 2 estimation of macro boundaries: 64th Ann. Internat. Mtg., SEG, Expanded Abstracts, SM6.3; 1334–1337.

Rietveld, W. E. A., and Thorbecke, J. W., 1994, Areal shot record technology; macro model estimation: DELPHI Volume V, Chapter 11, pages 255–304.

Timmerman, J. I. H., 1993, Removal of finite aperture artefacts: Ph.D. thesis, Delft University of Technology.

Wapenaar, C. P. A., On finite aperture artefacts:, Technical report, Amoco Production Company, 1991.

Contents